Locally Advanced Rectal Cancer: MR Imaging for Restaging after Neoadjuvant Radiation Therapy with Concomitant Chemotherapy Part II. What Are the Criteria to Predict Involved Lymph Nodes?[1]

Max J. Lahaye, MD, PhD
Geerard L. Beets, MD, PhD
Sanne M. E. Engelen, MD, PhD
Alfons G. H. Kessels, MD, MSc
Adriaan P. de Bruïne, MD, PhD
Herry W. S. Kwee, MD, PhD
Jos M. A. van Engelshoven, MD, PhD
Cornelis J. H. van de Velde, MD, PhD
Regina G. H. Beets-Tan, MD, PhD

Purpose: To prospectively determine diagnostic performance of predictive criteria for nodal restaging after radiation therapy with concomitant chemotherapy by using ultrasmall superparamagnetic iron oxide (USPIO)-enhanced magnetic resonance (MR) imaging in patients with rectal cancer.

Materials and Methods: After institutional review board approval and informed consent were obtained, 39 patients (24 men, 15 women; mean age, 64 years) with rectal cancer underwent USPIO-enhanced two-dimensional (2D) T2-weighted fast spin-echo, three-dimensional (3D) T1-weighted gradient-echo, and 3D T2*-weighted MR for restaging. Two observers evaluated nodes for border irregularity, short- and long-axis diameters, and estimated percentage of white region (<30%, 30%–50%, or >50%) within the node (3D T2*-weighted images). Ratio of the measured surface area of the white region within the black node to the measured surface area of the total node ($Ratio_A$) was calculated. Signal intensity (SI) in gluteus muscle (SI_{GM}) and in total node (SI_{TN}) were used to calculate SI_{TN}/SI_{GM} ratio. Histopathologic findings were reference standard. Receiver operating characteristic (ROC) curves were compared and interobserver agreement was determined.

Results: Lesion-by-lesion analysis was feasible in 201 lymph nodes. Area under the ROC curve (AUC) of border and short- and long-axis diameters for observer 1 were 0.85, 0.87, and 0.88 and for observer 2 were 0.70, 0.89, and 0.87, respectively. AUC for estimated percentage of white region within the node, $Ratio_A$, and SI_{TN}/SI_{GM} ratio for observer 1 were 0.98, 0.99, and 0.62 and for observer 2 were 0.97, 0.98, and 0.65, respectively. AUC for USPIO-enhanced MR criteria was significantly better than AUC for conventional MR criteria ($P < .01$). All criteria except border irregularity and SI_{TN}/SI_{GM} ratio showed high interobserver agreement ($\kappa > 0.79$).

Conclusion: The most reliable predictors for identifying benign nodes after radiation therapy with concomitant chemotherapy by using USPIO-enhanced MR imaging for restaging in patients with rectal cancer were estimated percentage of white region within the node and $Ratio_A$. Measurements on standard 2D T2-weighted fast spin-echo images versus primary staging results offer reasonably good accuracy to identify benign lymph nodes after therapy.

[1] From the Departments of Radiology (M.J.L., S.M.E.E., J.M.A.v.E., R.G.H.B.), Surgery (M.J.L., G.L.B., S.M.E.E.), Epidemiology (A.G.H.K.), and Pathology (A.P.d.B.), Maastricht University Medical Center, Maastricht, the Netherlands; Department of Pathology, Laurentius Hospital Roermond, Roermond, the Netherlands (H.W.S.K.); and Department of Surgery, Leiden University Medical Center, Leiden, the Netherlands (C.J.H.v.d.V.). Received August 4, 2008; revision requested September 23; revision received January 5, 2009; accepted January 27; final version accepted February 9. Supported in part by the Dutch Cancer Society grant UM 2004-3031. **Address correspondence to** R.G.H.B., Department of Radiology, Memorial Sloan-Kettering Cancer Center, 1275 York Ave, New York, NY 10021 (e-mail: *beetstar@mskcc.org*).

The standard treatment for locally advanced rectal cancer is preoperative radiation therapy with concomitant chemotherapy followed by standard resection of the rectum, with resection of surrounding organs when required. Neoadjuvant radiation therapy with concomitant chemotherapy has resulted in 15%–30% complete tumor response rates and almost 50% partial response rates, leading to improved resectability and local control. Eradication of tumor in involved lymph nodes also occurs, with a reported decline in the rate of tumors with malignant lymph nodes found at histopathologic evaluation from 40% before radiation therapy with concomitant chemotherapy to 25% after it (1–4). The clinical question that arises is thus: What do we do with a good response after radiation therapy with concomitant chemotherapy? As explained in the accompanying article by Dresen et al (part I) (5), patients with a good response could be selected for local excision when imaging would allow identification of a tumor remnant that is confined to the bowel wall and identification of disease without malignant lymph nodes. Assessment of the response to radiation therapy with concomitant chemotherapy in the tumor is discussed in the article by Dresen et al (5), and the present article focuses on the assessment of the response in the lymph nodes. Although a good response in the primary tumor generally is accepted to correspond with a good response in the lymph nodes, there are some conflicting findings in reports, with rates of involved nodes ranging from 1.7% to 17% in patients with a complete response in the primary tumor (6,7). This factor further indicates the need for a reliable imaging tool to assess the lymph node status after radiation therapy with concomitant chemotherapy.

Nodal staging in rectal cancer remains a problem for the radiologist. Investigators in two meta-analyses have shown that, for the identification of nodal disease on a patient-by-patient basis in primarily rectal cancer, all currently used imaging modalities lack sufficient accuracy for clinical decision making. The estimated sensitivity for endoluminal ultrasonography (US), magnetic resonance (MR) imaging, and computed tomography (CT) was 67%, 55%, and 66%, with corresponding specificity estimates of 78%, 74%, and 76% (8,9), respectively. All modalities rely heavily on the criterion of size, and size on its own is insufficient to reliably distinguish between malignant and benign lymph nodes in rectal cancer. Brown et al (10) showed that, among 3- and 5-mm large lymph nodes, the prevalence of malignant lymph nodes was 10% and 28%, respectively. MR imaging by using ultrasmall superparamagnetic iron oxide (USPIO) has shown promising results for detecting malignant nodes in the head and neck area, in the axilla, and in the pelvis (11). In a previous study, Lahaye et al (12) confirmed the good performance of USPIO-enhanced MR imaging for nodal staging in patients with primary rectal cancer, with a high sensitivity and specificity of approximately 95% for detection of malignant lymph nodes.

Secondary staging after radiation therapy with concomitant chemotherapy should be considered separately, as the behavior of a treated previously involved node may differ from that of a primary benign lymph node. A search of the literature revealed that only a few reports have been published on the accuracy of MR imaging methods to detect lymph node disease after radiation therapy with concomitant chemotherapy on a patient-by-patient basis, with accuracy rates of 65%–88% and sensitivity and specificity values varying from 33% to 82% and from 68% to 95%, respectively (13–16). To our knowledge, there have been no lesion-by-lesion studies on lymph nodes in rectal cancer patients after radiation ther-

Advances in Knowledge

- For predicting lymph node involvement after radiation therapy with concomitant chemotherapy, a 30% estimated percentage of the white region within the node on ultrasmall superparamagnetic iron oxide–enhanced MR images is the most reliable criterion, with a high area under the receiver operating characteristic curve (AUC) of 0.99.
- In contrast to primary staging, standard MR images with short- and long-axis diameter criteria offer a reasonably good accuracy for predicting involved nodes after radiation therapy with concomitant chemotherapy, with an AUC of 0.89.

Implication for Patient Care

- An MR image for restaging after radiation therapy with concomitant chemotherapy in rectal cancer patients could be a useful diagnostic tool for the identification of patients without nodal involvement.
- This diagnostic tool could allow clinicians to consider transanal local excision in good responders after radiation therapy with concomitant chemotherapy, with less morbidity and mortality than after standard surgery.

Published online before print
10.1148/radiol.2521081364

Radiology 2009; 252:81–91

Abbreviations:
AUC = area under the ROC curve
NPV = negative predictive value
PPV = positive predictive value
$Ratio_A$ = ratio of the measured surface area of the white region within the black node to the measured surface area of the total node
ROC = receiver operating characteristic
SI = signal intensity
SI_{GM} = SI of the gluteus muscle
SI_{TN} = SI of the total node
3D = three-dimensional
2D = two-dimensional
USPIO = ultrasmall superparamagnetic iron oxide

Author contributions:
Guarantors of integrity of entire study, G.L.B., H.W.S.K., R.G.H.B.; study concepts/study design or data acquisition or data analysis/interpretation, all authors; manuscript drafting or manuscript revision for important intellectual content, all authors; manuscript final version approval, all authors; literature research, M.J.L., S.M.E.E., H.W.S.K., J.M.A.v.E., R.G.H.B.; clinical studies, M.J.L., G.L.B., S.M.E.E., H.W.S.K., J.M.A.v.E., R.G.H.B.; statistical analysis, M.J.L., A.G.H.K., H.W.S.K., R.G.H.B.; and manuscript editing, M.J.L., G.L.B., S.M.E.E., A.G.H.K., A.P.d.B., H.W.S.K., J.M.A.v.E., R.G.H.B.

See Materials and Methods for pertinent disclosures.

See also the article by Dresen et al in this issue.

apy with concomitant chemotherapy that could provide criteria and no studies on USPIO-enhanced MR imaging to date. It is not known whether our previously established criteria for the prediction of involved nodes in primarily untreated rectal cancer also apply after radiation therapy with concomitant chemotherapy: the estimated percentage of the white region (the region with no USPIO uptake) within the black node and the ratio of the measured surface area of the white region within the black node to the measured surface area of the total node ($Ratio_A$) on T2*-weighted images.

The purpose of this study was therefore to prospectively determine the diagnostic performance of predictive criteria for USPIO-enhanced MR imaging in nodal restaging after radiation therapy with concomitant chemotherapy in patients with rectal cancer.

Materials and Methods

This study was partly financed by the Dutch Cancer Society (the multicenter part of the study). Guerbet Laboratories (Roissy, France) only provided the USPIO contrast agent and had no control of the data. The authors had full control of the data and information submitted for publication.

Patients

Between February 2003 and January 2008, a multicenter prospective rectal cancer project included 296 patients with rectal cancer. The main aim was to study local control after MR imaging–based differentiated treatment. The institutional review board approved the study. Written informed consent was obtained from all patients. Exclusion criteria were pregnancy, age younger than 18 years, mental disability precluding informed consent, and contraindications for MR imaging (pacemaker, neurostimulator, insulin pump, certain vascular clips such as those used in brain surgery, cochlear implants, metallic splinters in the eye, any other metal implant not securely fixed, or an electronic device).

In this large prospective project, all patients underwent USPIO-enhanced MR imaging for primary staging and were stratified into low-, intermediate-, and high-risk groups for a local recurrence on the basis of the MR imaging findings. The tumors in the high-risk group were defined as tumors with a threatened or involved circumferential resection margin, tumors with more than three involved lymph nodes (N2 status), and any T3 or N1 distal tumor. The recommended treatment for these tumors was radiation therapy with concomitant chemotherapy (chemotherapy that was based on fluorouracil [Fluracedyl; Teva Pharmachemie, Haarlem, the Netherlands] with 1.8 Gy of radiation therapy for 28 days), followed by resection 6–8 weeks after completion of radiation therapy with concomitant chemotherapy. Most of these patients also underwent a second restaging with USPIO-enhanced MR imaging 4–6 weeks after completion of the radiation therapy with concomitant chemotherapy and 1–2 weeks (mean, 4 days; range, 1–14 days) before resection.

For the present study, which addresses the diagnostic performance of predictive criteria for USPIO-enhanced MR imaging in nodal restaging after radiation therapy with concomitant chemotherapy, patients were eligible for inclusion when *(a)* they were treated with radiation therapy with concomitant chemotherapy; *(b)* they underwent restaging with USPIO-enhanced MR imaging; and *(c)* they underwent resection, which provided the reference standard of histopathologic findings. The sample size required for the present study, calculated as shown in the Statistical Analysis section, was set as the harvest of at least 40 malignant nodes. At the start of the project, it was therefore decided to include patients for the lesion-by-lesion analysis until this number was achieved. At the end of the project, 95 patients overall had received radiation therapy with concomitant chemotherapy. The required number of malignant nodes was obtained after including the first 39 consecutive eligible patients. These 24 men and 15 women, with a mean age of 64 years (range, 35–87 years) form the basis of the present study.

Ultrasmall Superparamagnetic Iron Oxide

The USPIO MR contrast agent (Sinerem; Guerbet Laboratories) used in this study consists of low–molecular-weight iron oxide coated with dextran. This contrast agent is supplied as a powder in a glass vial containing 210 mg and must be reconstituted by using 10 mL of normal saline. A dose of 0.13 mL per kilogram of body weight (2.6 mg of iron per kilogram) of the reconstituted solution was diluted in 100 mL of normal saline. The contrast agent was administered intravenously in the preparation room of the MR unit within a period of approximately 45 minutes by means of a slow-drip infusion with a microfilter. During infusion, all patients were closely monitored for any adverse effects. The most common adverse events described in the literature for this contrast agent are headache (2.9%), back pain (3.3%), and urticaria (2.4%). Administration was completed 24–36 hours before MR imaging.

The variation of signal intensity (SI) within a node on MR images can be explained on the basis of the concentration of nanoparticles in a particular region in the node. The nanoparticles cause a decrease in SI within the node owing to susceptibility artifacts on T2*-weighted images. Nanoparticles are taken up by macrophages located in the node (17). The part of the lymph node involved with tumor will show no SI decrease because of the replacement of macrophages by tumor cells and thus will be depicted as a white region.

MR Imaging

After radiation therapy with concomitant chemotherapy, MR imaging was performed 24–36 hours after administration of the contrast agent USPIO. No MR imaging before contrast agent administration was performed, because no benefit was shown from unenhanced MR imaging in a published series of patients in whom USPIO was used (18). MR imaging was performed with a 1.5-T system (Gyroscan, Power-Trak NT 6000; Philips Medical Systems, Best, the Netherlands) and a 1.0-T system (Magnetom Impact Expert; Siemens, Erlangen, Germany). Patients were placed in the magnet in the feet-first supine position. The entire pelvis was imaged with standard two-dimensional (2D) T2-weighted

fast spin-echo sequences in three planes: sagittal, axial, and coronal. The MR image obtained in the sagittal plane was used as a reference image to plan the acquisition of MR images in the axial and coronal planes so that they would be exactly perpendicular and parallel to the primary tumor in the rectal wall, respectively.

To evaluate the morphologic uptake pattern of the iron oxide particles within the nodes, three-dimensional (3D) T2*-weighted images were used. The 3D T1-weighted gradient-echo sequence was performed in exactly the same obliquity to serve as an anatomic template for better depiction of small lymph nodes. The detailed pulse sequence parameters are provided in Table 1. Patients did not receive bowel or other preparation. Total imaging time was 42–50 minutes.

Image Analysis

In this study, MR images obtained after radiation therapy with concomitant chemotherapy were analyzed independently by two observers (R.G.H.B. [observer 1] and M.J.L. [observer 2], with experience in reading approximately 3000 and approximately 300 pelvic MR images, respectively). The MR images obtained before radiation therapy with concomitant chemotherapy were available for review, reflecting the daily practice. Both observers were blinded to each other's results and to the findings at histopathologic evaluation. Both observers prospectively evaluated each node on standard 2D T2-weighted fast spin-echo images first for the following items: border (sharp, indistinct, or spiculated) and short- and long-axis diameters.

Then, the 3D T2*-weighted images were evaluated for each node for the following criteria: The percentage of the area with no uptake (white region) within the node after radiation therapy with concomitant chemotherapy was estimated and categorized as less than 30%, 30%–50%, or more than 50% (Fig 1). Hereafter, this criterion is referred to as the estimated percentage of the white region within the node. In addition to this visual assessment, the proportion of white region within the node was also quantitatively measured. The surface area of white region within the node and the surface area of the total node were determined on axial 3D T2*-weighted images by using regions of interest at the section with greatest visualized diameter. The ratio of the measured surface area of the white region within the node to the measured surface area of the total node ($Ratio_A$) was calculated quantitatively for both observers. $Ratio_A$ was not categorized.

In addition, the SI of the total node (SI_{TN}) and the SI of the gluteus muscle (SI_{GM}) were measured after radiation therapy with concomitant chemotherapy by placing regions of interest. These SI values were used to calculate the SI_{TN}/SI_{GM} ratio for both observers.

Table 1

MR Sequences and Parameters

Sequences and Parameters	1.0-T Unit	1.5-T Unit
3D T1-weighted gradient echo		
Repetition time/echo time (msec)	15/7	10/4.60
Section thickness (mm)	2	1
Flip angle (degrees)	15	15
Matrix	256 × 256	512 × 512
No. of sections	102	200
3D T2* weighted		
Repetition time/echo time (msec)	15/7	23/18.41
Section thickness (mm)	2	1.25
Flip angle (degrees)	20	20
Matrix	256 × 256	384 × 512
No. of sections	106	200

The observer with the higher level of experience, observer 1, also prospectively recorded on an anatomic map the localization of each visible lymph node depicted on T2*-weighted MR images after radiation therapy with concomitant chemotherapy. This anatomic map was used as a template for matching each node recorded by observer 1 with the nodes found by the pathologist, as well as for matching each node with the nodes recorded by observer 2. All images were evaluated by using a picture archiving and communication system workstation (Carestream PACS, version 10; Kodak, Rochester, NY).

Surgical Procedure and Histopathologic Evaluation

The standard surgical procedure was total mesorectal excision, as described by Heald (19). In some patients, a more extensive en bloc resection of adjacent structures or organs was required on the basis of the findings on the MR image used for primary staging. The histopathologic evaluation was standardized: The specimen was inked and fixed in formalin for 24–48 hours. The specimen was then sectioned every 5 mm transversely and, thus, perpendicularly to the mesorectum. A careful search for lymph nodes was made in each histopathologic tissue slice by dedicated pathologists (A.P.d.B. and H.W.S.K., both with more than 10 years of experience). Each harvested lymph node was processed according to standard methods and stained with hematoxylin-eosin. The pathologists, who were blinded to the radiologic findings, reported the status of each lymph node. Each lymph node was matched to the corresponding node that was visible on the MR images by using the anatomic map as a template (M.J.L., S.M.E.E., and R.G.H.B.). This procedure was possible because of specific characteristics, such as the size of the lymph node and the position of the lymph node in relation to the rectal wall, small blood vessels, mesorectal fascia, tumor, and other lymph nodes. In this manner, accurate lesion-by-

Figure 1

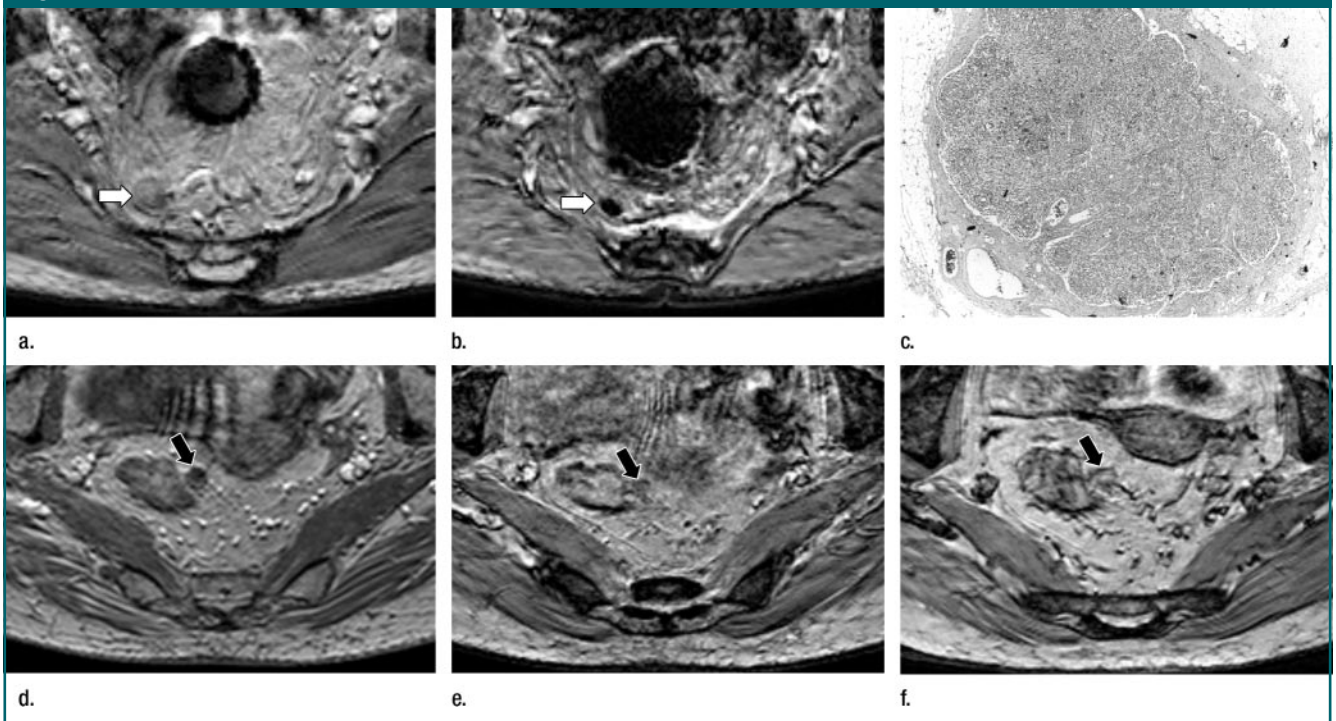

Figure 1: USPIO-enhanced 3D T2*-weighted axial MR images in 36-year-old male rectal cancer patient **(a)** before and **(b)** after radiation therapy with concomitant chemotherapy. On **a**, node remains white (arrow), which indicates no iron uptake and that it is malignant. On **b**, same node shows low SI, indicating iron uptake, and suggests eradication of tumor. **(c)** Histopathologic slice shows node was benign. This finding suggests that nodes that become free of tumor after therapy reacquire their ability to take up iron oxide. (Hematoxylin-eosin; original magnification, × 2.5.) **(d–f)** Axial images in 65-year-old female rectal cancer patient. **(d)** Three-dimensional T1-weighted gradient-echo MR image of large lymph node (arrow, also **e** and **f**) close to rectal wall. **(e)** USPIO-enhanced 3D T2*-weighted MR image of rectal cancer of same node, which remains white and indicates no iron uptake. **(f)** MR image after therapy shows same node, which remains white and means the node is still malignant. At histopathologic evaluation, node was malignant.

lesion analysis for mesorectal lymph nodes could be performed (Fig 2). In cases in which matching of the nodes with high accuracy was not possible, that factor was recorded as such, and these nodes were excluded from the analyses. When available, the histopathologic details of the nodes for which matching was not possible were recorded.

Statistical Analysis

The diagnostic accuracy was assessed in a per-node lesion-by-lesion analysis. On the basis of the results of a pilot study at Maastricht University Medical Center, Maastricht, the Netherlands, we expected a sensitivity of 99%. Forty malignant lymph nodes are needed to reject with a power of 94% that the lower limit of the 95% confidence interval for sensitivity of USPIO-enhanced MR imaging is 89% or lower. Patients were therefore included until a total of 40 malignant lymph nodes were harvested at histopathologic evaluation.

To determine the diagnostic performance of each criterion, receiver operating characteristic (ROC) curves were constructed and area under the ROC curve (AUC) and 95% confidence intervals were calculated. The constructed ROC curves were compared, and *P* values were constructed by using the method of DeLong et al (20). For the calculation of corresponding sensitivity, specificity, positive predictive value (PPV), and negative predictive value (NPV), the variables were dichotomized at the most optimal cutoff point determined at the highest NPV still with a reasonable PPV. To determine the interobserver agreement, weighted κ values (21,22) were calculated for the ordinal variables and intraclass correlations for interval-scaled variables (23), all with their 95% confidence intervals. Agreement was determined ($\kappa < 0$, poor agreement; $\kappa = 0$–0.20, slight agreement; $\kappa = 0.21$–0.40, fair agreement; $\kappa = 0.41$–0.60, moderate agreement; $\kappa = 0.61$–0.80, substantial agreement; and $\kappa = 0.81$–1.00, almost perfect agreement) (24). All analyses, with the exception of the κ and *P* value analyses, were performed by using a statistical software program (SPSS, version 12.0.1, 2003; SPSS, Chicago, Ill). The κ and *P* value analyses were performed by using other software (Stata, release 9; StataCorp, College Station, Tex). The statistical analysis was performed by a statistician (A.G.H.K.).

Results

No adverse events related to the USPIO infusion were observed. Observer 1

identified and evaluated 320 mesorectal nodes in 39 patients on USPIO-enhanced MR images obtained after radiation therapy with concomitant chemotherapy. After surgical resection, 325 nodes were found at histopathologic evaluation; 40 lymph nodes were malignant and 285 lymph nodes were benign. The average number of nodes found at histopathologic evaluation per patient was 8.3 (range, 1–16 nodes). At histopathologic evaluation, 28 patients had no malignant mesorectal nodes (ypN0 lesions), six patients had zero to three malignant nodes (ypN1 lesions), and five patients had four or more malignant lymph nodes (ypN2 lesions).

Of the 325 nodes harvested at histopathologic evaluation, 201 could be accurately matched with MR imaging findings, as could all 40 malignant lymph nodes found at histopathologic evaluation. The remaining 124 nodes harvested at histopathologic evaluation could not be matched with MR imaging findings with great certainty and therefore were excluded from the analysis (Figs 3, 4). These 124 nonmatched lymph nodes were all benign at histopathologic evaluation, and almost all of them were small (<2 mm). One hundred ten "nodes" that were depicted on MR images could not be matched with histopathologic findings with certainty. On MR images, these nodes were all staged as benign nodes. Three reasons that a node seen on an MR image could not be matched with histopathologic findings follow: First, small blood vessels or small areas of fibrosis could be interpreted as lymph nodes on MR images. Second, the nodes seen on MR images were real lymph nodes but could not be found at histopathologic evaluation. Third, the nodes were also found during histopathologic evaluation but could not be matched with certainty.

The mean short- and long-axis diameters at histopathologic evaluation of the 201 matched lymph nodes were 3.2 mm (range, 1–13 mm) and 4.6 mm (range, 1.5–19 mm), respectively (Fig 5). Quantitative measurement on 3D T2*-weighted MR images was feasible in all matched nodes, even in the small nodes because the blooming artifact of the iron oxide on the T2*-weighted images was large enough for quantification of SI. Each node evaluated by observer 1 and matched with histopathologic findings was also identified and evaluated by observer 2.

Figure 2

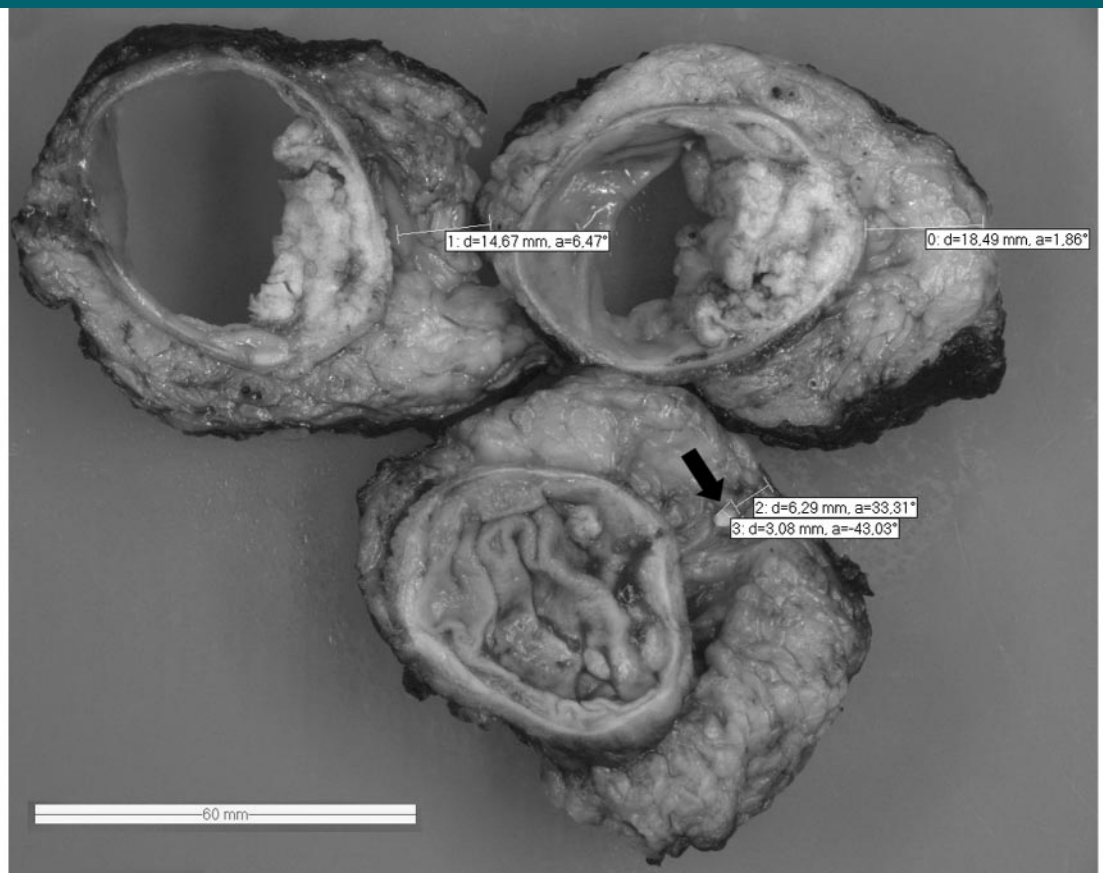

Figure 2: Three histopathologic slices of rectal specimen with 3-mm lymph node (arrow) and several measurements (ie, distance from node to tumor and circumferential resection margin, needed for an accurate lesion-by-lesion analysis). *a* = angle, *d* = distance, *0–3* = number of measurements.

Figure 3

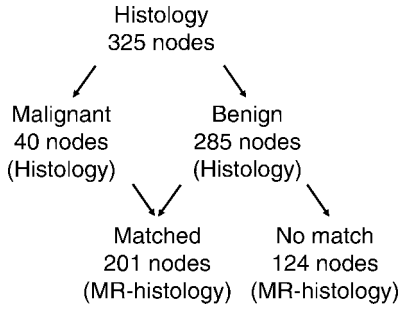

Figure 3: Flowchart of lymph nodes found at histopathologic evaluation (*Histology*) in rectal cancer patients after radiation therapy with concomitant chemotherapy. *MR-histology* indicates that nodes depicted on MR images were matched with nodes found at histopathologic evaluation.

Figure 4

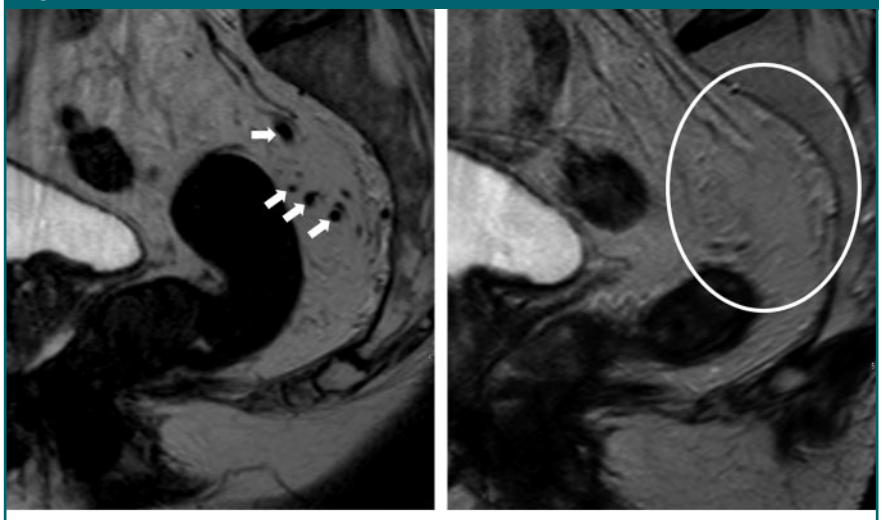

a. b.

Figure 4: **(a)** Two-dimensional T2-weighted fast spin-echo sagittal MR image in 61-year-old male rectal cancer patient before radiation therapy with concomitant chemotherapy shows multiple small and borderline (≤5 mm) nodes (arrows). **(b)** Same view in same patient after therapy shows that small mesorectal lymph nodes disappeared (oval).

Figure 5

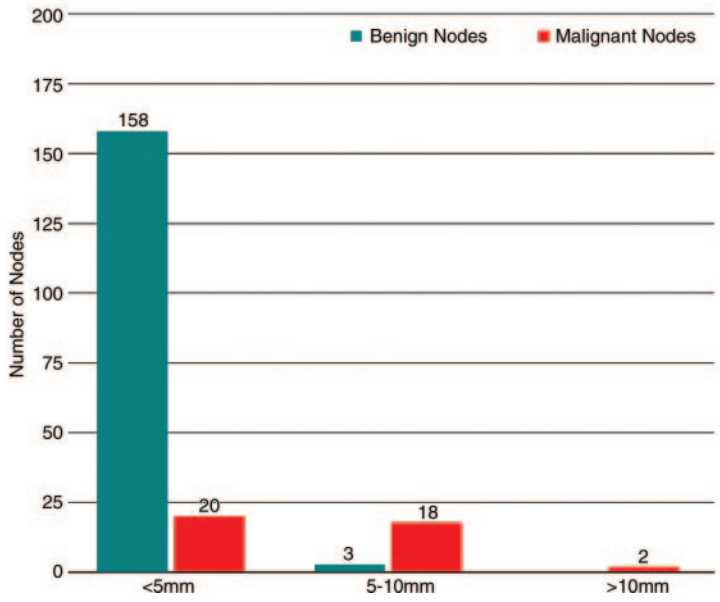

Figure 5: Graph shows number of lymph nodes according to short-axis diameter of smaller than 5 mm, 5–10 mm, and larger than 10 mm.

Diagnostic Performance

The AUC for the short- and long-axis diameters of the nodes on 2D T2-weighted fast spin-echo images was 0.87 and 0.88 for observer 1 and 0.89 and 0.87 for observer 2, respectively. The optimal cutoff value of the short-axis diameter was 3.3 mm, with corresponding sensitivity and specificity for the detection of malignant nodes of 85% and 78%, respectively, for observer 2. The optimal cutoff value of the long-axis diameter was 4.8 mm, with corresponding sensitivity and specificity for the detection of malignant nodes of 82% and 82%, respectively (Table 2, Fig 6). The AUC for a sharp, distinct, or spiculated border on 2D T2-weighted fast spin-echo images was 0.85 and 0.70 for observers 1 and 2, respectively.

The AUC of the estimated percentage of the white region within the node for the prediction of the nodal status on 3D T2*-weighted images was 0.98 for observer 1 and 0.97 for observer 2. When the estimated percentage of the white region within the node was more than 30%, the sensitivity and specificity for detection of malignant nodes on MR images obtained after radiation therapy with concomitant chemotherapy were 100% and 95%, respectively, for observer 2 (Table 2, Fig 7).

The AUC of $Ratio_A$ for the prediction of the nodal status was 0.99 for observer 1 and 0.98 for observer 2 on 3D T2*-weighted images. The most clinically relevant cutoff value for $Ratio_A$ was 0.34. When $Ratio_A$ was 0.34, the sensitivity and specificity for the prediction of malignant nodes were 100% and 96%, respectively, for observer 1. The AUC of the SI_{TN}/SI_{GM} ratio was 0.62 for observer 1 and 0.65 for observer 2. The AUC of the USPIO-enhanced MR imaging criteria of the estimated percentage of the white re-

Table 2

Diagnostic Performance of Criteria for Prediction of Malignant Nodes in Lesion-by-Lesion Analysis

A: On 2D T2-weighted Fast Spin-Echo MR Images

	Observer 1			Observer 2		
Statistic	Short-axis Diameter	Long-axis Diameter	Border	Short-axis Diameter	Long-axis Diameter	Border
AUC*	0.87 (0.82, 0.94)	0.88 (0.81, 0.93)	0.85 (0.76, 0.94)	0.89 (0.84, 0.95)	0.87 (0.81, 0.94)	0.70 (0.60, 0.80)
Accuracy (%)†	81 [(32 + 130)/201]	82 [(33 + 132)/201]	90 [(29 + 151)/201]	80 [(34 + 126)/201]	78 [(33 + 124)/201]	67 [(26 + 109)/201]
Sensitivity (%)†	80 [32/(32 + 8)]	82 [33/(33 + 7)]	74 [29/(29 + 10)]	85 [34/(34 + 6)]	82 [33/(33 + 7)]	65 [26/(26 + 14)]
Specificity (%)†	81 [130/(130 + 31)]	82 [132/(132 + 29)]	93 [151/(151 + 11)]	78 [126/(126 + 35)]	77 [124/(124 + 37)]	68 [109/(109 + 52)]
PPV (%)†	51 [32/(32 + 31)]	53 [33/(33 + 29)]	72 [29/(29 + 11)]	49 [34/(34 + 35)]	47 [33/(33 + 37)]	33 [26/(26 + 52)]
NPV (%)†	94 [130/(130 + 8)]	95 [132/(132 + 7)]	94 [151/(151 + 10)]	95 [126/(126 + 6)]	95 [124/(124 + 7)]	89 [109/(109 + 14)]

B: On USPIO-enhanced 3D T2*-weighted MR Images

	Observer 1			Observer 2		
Statistic	Estimated Percentage	$Ratio_A$	SI_{TN}/SI_{GM} Ratio	Estimated Percentage	$Ratio_A$	SI_{TN}/SI_{GM} Ratio
AUC*	0.98 (0.96, 1.00)	0.99 (0.99, 1.00)	0.62 (0.51, 0.73)	0.97 (0.95, 0.99)	0.98 (0.96, 1.00)	0.65 (0.55, 0.76)
Accuracy (%)†	96 [(39 + 153)/201]	97 [(40 + 155)/201]	54 [(22 + 87)/201]	96 [(40 + 153)/201]	95 [(40 + 151)/201]	56 [(21 + 92)/201]
Sensitivity (%)†	98 [39/(39 + 1)]	100 [40/(40 + 0)]	55 [22/(22 + 18)]	100 [40/(40 + 0)]	100 [40/(40 + 0)]	52 [21/(21 + 19)]
Specificity (%)†	95 [153/(153 + 8)]	96 [155/(155 + 6)]	54 [87/(87 + 74)]	95 [153/(153 + 8)]	94 [151/(151 + 10)]	57 [92/(92 + 69)]
PPV (%)†	83 [39/(39 + 8)]	87 [40/(40 + 6)]	23 [22/(22 + 74)]	83 [40/(40 + 8)]	80 [40/(40 + 10)]	23 [21/(21 + 69)]
NPV (%)†	99 [153/(153 + 1)]	100 [155/(155 + 0)]	83 [87/(87 + 18)]	100 [153/(153 + 0)]	100 [151/(151 + 0)]	83 [92/(92 + 19)]

Note.—Estimated percentage is the estimated percentage of the white region within the node.

* Numbers in parentheses are 95% confidence intervals.

† Calculations with raw data in brackets were used to determine percentages.

Figures 6, 7

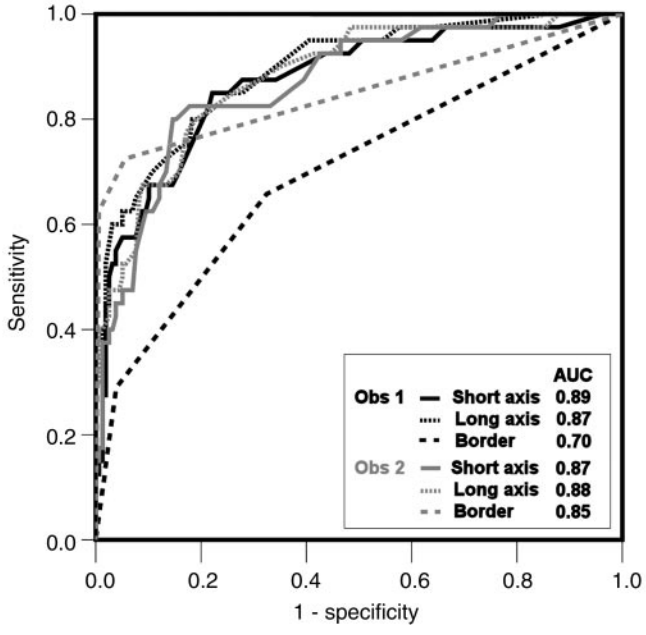

Figure 6: ROC curve and AUC for observers 1 and 2 for detection of malignant lymph nodes by using short- and long-axis diameters and border of lymph node.

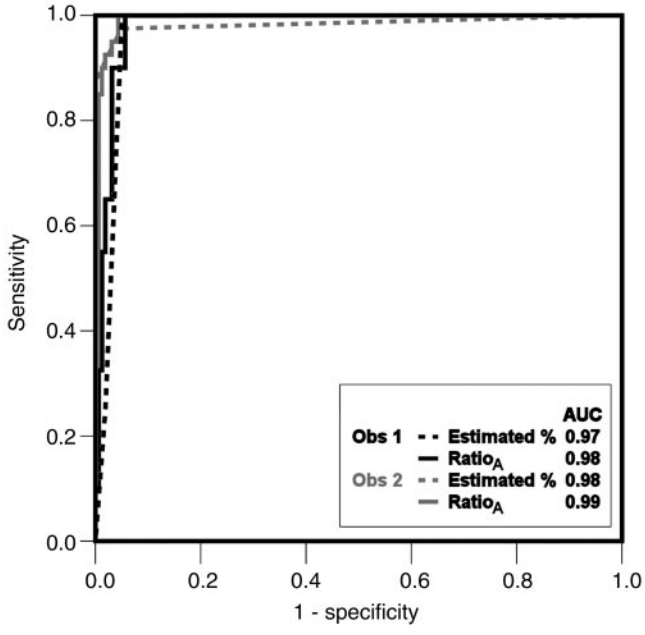

Figure 7: ROC curve and AUC for observers 1 and 2 for detection of malignant lymph nodes by using estimated percentage of white region within the node and $Ratio_A$.

gion within the node and $Ratio_A$ was significantly better than the AUC of the conventional size measurements for both observers ($P < .01$ for all comparisons).

Intraclass Correlation and Interobserver Agreement

The intraclass correlation for observers 1 and 2 for the short- and long-axis diameters, $Ratio_A$, and the SI_{TN}/SI_{GM} ratio on MR images obtained after radiation therapy with concomitant chemotherapy were 0.94, 0.97, 0.83, and 0.73, respectively. Generally, the interobserver agreement was good to excellent. There was higher agreement between both observers for $Ratio_A$ and short- and long-axis diameters than for the SI_{TN}/SI_{GM} ratio.

The interobserver agreement (κ value) for the estimated percentage of the white region within the node between observers 1 and 2 was substantial (0.79), whereas that for the border was only fair (0.36).

Discussion

Our study shows that, in patients with rectal cancer treated with neoadjuvant radiation therapy with concomitant chemotherapy, the most accurate predictors for malignant nodes on an MR image obtained for restaging by using a lymph node–specific USPIO contrast agent were both the estimated percentage of the white region within the node and $Ratio_A$, with an AUC of 0.98 and 0.99, respectively, for the more experienced reader (observer 1) and an AUC of 0.97 and 0.98, respectively, for the less experienced reader (observer 2). With a low prevalence of malignant nodes after radiation therapy with concomitant chemotherapy of about 20%, the high sensitivity leads to an NPV of almost 100%, irrespective of the experience of the radiologist. Respective measurements of short- and long-axis diameters of the node on standard 2D T2-weighted fast spin-echo images were significantly less reliable predictors for malignant nodes, but still with a good AUC of 0.87 and 0.88 for observer 1 and 0.89 and 0.87 for observer 2. Border irregularity and SI measurements were unreliable criteria for detection of malignant nodes.

In contrast to the results of a previous study about primary staging with MR imaging (12), where size criteria were not reliable enough with an AUC of 0.75, size criteria after radiation therapy with concomitant chemotherapy provide a higher AUC of 0.85–0.90. The sensitivity and specificity are approximately 80%, and with a low prevalence of nodal disease after radiation therapy with concomitant chemotherapy of 20%, these values result in a high NPV both for the more experienced and less experienced readers. The specificity of 80% in this group of patients results in a PPV of only 50%, resulting in overstaging, a problem that is well known (16,25). There are several observations that could explain the better performance of size criteria after radiation therapy with concomitant chemotherapy than for primary staging. Small nodes often cause interpretation difficulties on standard 2D T2-weighted fast spin-echo images, and after radiation therapy with concomitant chemotherapy, the number of lymph nodes harvested during histopathologic evaluation is reduced by 30% (14,26). This factor could lead to fewer interpretation errors in small nodes, improving the accuracy. In addition, the radiologist can compare the images obtained after radiation therapy with concomitant chemotherapy with the images obtained before it. The knowledge that the lymph nodes that are still malignant after radiation therapy with concomitant chemotherapy are initially the larger nodes and that initially small malignant nodes often are benign after radiation therapy with concomitant chemotherapy can increase the confidence of the radiologist in judging the smaller lymph nodes as benign.

The researchers in two studies have addressed USPIO-enhanced MR imaging in primary nodal staging (without radiation therapy with concomitant chemotherapy): The study by Koh et al (27) describes the initial observations about a range of patterns of contrast enhancement to discriminate between malignant and nonmalignant lymph nodes. A study from our research group (12) demonstrated that a simple estimation or measurement of the white region within the node is a reliable tool in primary nodal staging. Our present study shows that these criteria are also valid in a setting after radiation therapy with concomitant chemotherapy. Apparently, tumoral nodes that show no uptake of nanoparticles before radiation therapy with concomitant chemotherapy regain their capability for uptake of the USPIO contrast agent when the tumor is eradicated by using radiation therapy with concomitant chemotherapy. This finding suggests that tumor cells are replaced by normal lymphoid tissue with macrophages, which are responsible for the uptake of nanoparticles of iron oxide (18).

Although studies on individual lymph nodes with a lesion-by-lesion analysis are valuable to establish radiologic criteria, the assessment of the nodal status on a patient-by-patient basis is clinically more relevant for decision making. The results of the clinical data analysis in our larger multicenter cohort study show that, on a patient-by-patient basis, the sensitivity of USPIO-enhanced MR imaging for detection of malignant lymph nodes after radiation therapy with concomitant chemotherapy is close to 90%, with a specificity of 80% (28). In a group of patients with a prevalence of nodal disease of 29%, this finding leads to a clinically useful NPV of 95% with a lower PPV of 65% (S. M. E. Engelen, MD, PhD, R. G. H. Beets-Tan, MD, PhD, M. J. Lahaye, MD, PhD, et al, unpublished data, March 27, 2009). Researchers in most other imaging studies on the prediction of nodal staging after radiation therapy with concomitant chemotherapy report results of analyses on a patient-by-patient basis, with unenhanced MR imaging showing sensitivity and specificity values, respectively, of 33%–82% and 68%–95%, with NPVs of 81%–93% (13–15). In reports on nodal restaging with endoluminal US and CT after radiation therapy with concomitant chemotherapy, investigators show only moderate accuracy values of 0.61 and 0.62, respectively, which are comparable to those at primary nodal staging (15). Investigators in studies on the use of fluorine 18 (^{18}F) fluorodeoxyglucose positron emission tomography (PET) in restaging after radiation therapy with concomitant chemotherapy focus mostly on the accuracy to detect complete responders or to evaluate the response, and

data on the prediction of nodal status are scarce. The sensitivity to detect a complete response (in both the primary tumor and the lymph nodes) is 45%, with a specificity of 79% (28,29). In the prediction of the nodal status in primary rectal cancer, ^{18}F fluorodeoxyglucose PET performs poorly, with a sensitivity of 21%–29%, and it is not expected to perform much better after radiation therapy with concomitant chemotherapy (30,31). After radiation therapy with concomitant chemotherapy, the foci of tumor in malignant nodes are expected to be even smaller than in untreated rectal cancer, and detecting small volumes of tumor is a well-known limitation of ^{18}F fluorodeoxyglucose PET.

A limitation of our study was the relatively high number of nodes at histopathologic evaluation that could not be matched with certainty with MR imaging findings. To not pollute the analysis with faulty matched nodes, lymph nodes were included only when both the radiologist and the pathologist were confident about the matching. After radiation therapy with concomitant chemotherapy, most benign lymph nodes become smaller, and because lymph nodes smaller than 2 mm are difficult to depict with MR imaging and can easily be misinterpreted as small blood vessels or small areas of fibrosis, many of these small nodes could not be matched. Reassuring is the fact that the nodes seen on MR images that could not be matched with histopathologic findings all were judged to be benign on MR images and, most important, that all the nodes detected at histopathologic evaluation that could not be matched with MR imaging findings were all proved to be benign at histopathologic evaluation.

Another drawback was that, in Europe, the application for a marketing authorization at the Committee for Medical Products for Human Use for USPIO recently has been withdrawn by the manufacturer, whereas in the United States the approval by the Food and Drug Administration is still pending. Should USPIO not be marketed, our study will have shown that, for lymph node staging after radiation therapy with concomitant chemotherapy, the accuracy of the size criteria can be improved with a lymph node–specific contrast agent. This finding could stimulate the search for other reliable contrast agents.

Preoperative radiation therapy with concomitant chemotherapy is now widely recognized as the treatment of choice for locally advanced rectal cancer. The majority of tumors become smaller, with complete remission rates of the primary tumor in 15%–30% and eradication of tumor in lymph nodes in almost one-half of patients with involved nodes. These good responses challenge the classic concept that the complete area of the initial tumor and mesorectum should be entirely removed irrespective of the response to radiation therapy with concomitant chemotherapy. In patients with a small tumor remnant in the bowel wall and without lymph node involvement, transanal local excision could result in good oncologic control with less morbidity and mortality, as demonstrated in a recent study of patients treated as such (32). Even more controversial is a wait-and-see policy in complete responses in both the primary tumor and the lymph nodes (33). To select patients for local excision after radiation therapy with concomitant chemotherapy, both a residual (ypT0–2) tumor limited to the bowel wall and a negative lymph node (ypN0) status are essential. In the accompanying part I article by Dresen et al (5), they have shown that MR imaging can reliably be used to detect a tumor remnant limited to the bowel wall, and in this part II article, we have shown that MR imaging with a lymph node–specific contrast agent (USPIO) can help to distinguish benign from malignant lymph nodes after radiation therapy with concomitant chemotherapy. Clinical studies for evaluation of the outcome of MR imaging–based selection of good responders after radiation therapy with concomitant chemotherapy for local excision are needed now.

In conclusion, the most reliable predictors for identifying benign lymph nodes in patients with locally advanced rectal cancer on a USPIO-enhanced MR image for restaging after radiation therapy with concomitant chemotherapy are the estimated percentage of the white region within the node and $Ratio_A$. In contrast to the results with MR imaging for primary staging, size measurements on standard 2D T2-weighted fast spin-echo images offer a reasonably good accuracy to identify benign nodes after radiation therapy with concomitant chemotherapy. The high agreement in both criteria between a more experienced and a less experienced reader indicates reproducibility of the readings in a general setting. Our study results suggest that MR imaging for restaging after radiation therapy with concomitant chemotherapy could be a useful diagnostic tool for the selection of good responders with ypN0 status who could be treated with less invasive transanal local excision of the residual tumor.

References

1. Lehnert T, Methner M, Pollok A, Schaible A, Hinz U, Herfarth C. Multivisceral resection for locally advanced primary colon and rectal cancer: an analysis of prognostic factors in 201 patients. Ann Surg 2002;235:217–225.
2. Sauer R, Becker H, Hohenberger W, et al. Preoperative versus postoperative chemoradiotherapy for rectal cancer. N Engl J Med 2004;351:1731–1740.
3. Govindarajan A, Coburn NG, Kiss A, Rabeneck L, Smith AJ, Law CH. Population-based assessment of the surgical management of locally advanced colorectal cancer. J Natl Cancer Inst 2006;98:1474–1481.
4. Reerink O, Verschueren RC, Szabo BG, Hospers GA, Mulder NH. A favourable pathological stage after neoadjuvant radiochemotherapy in patients with initially irresectable rectal cancer correlates with a favourable prognosis. Eur J Cancer 2003;39:192–195.
5. Dresen RC, Beets GL, Rutten HJT, et al. Locally advanced rectal cancer: MR imaging for restaging after neoadjuvant radiation therapy with concomitant chemotherapy. I. Are we able to predict tumor confined to the rectal wall? Radiology 2009;252(1):XXX–XXX.
6. Coco C, Manno A, Mattana C, et al. The role of local excision in rectal cancer after complete response to neoadjuvant treatment. Surg Oncol 2007;16(suppl 1):S101–S104.
7. Hughes R, Glynne-Jones R, Grainger J, et al. Can pathological complete response in the primary tumour following pre-operative pelvic chemoradiotherapy for T3-T4 rectal cancer predict for sterilisation of pelvic lymph nodes, a low risk of local recurrence and the appropriateness of local excision? Int J Colorectal Dis 2006;21:11–17.

8. Lahaye MJ, Engelen SM, Nelemans PJ, et al. Imaging for predicting the risk factors—the circumferential resection margin and nodal disease—of local recurrence in rectal cancer: a meta-analysis. Semin Ultrasound CT MR 2005;26:259–268.

9. Bipat S, Glas AS, Slors FJ, Zwinderman AH, Bossuyt PM, Stoker J. Rectal cancer: local staging and assessment of lymph node involvement with endoluminal US, CT, and MR imaging—a meta-analysis. Radiology 2004; 232:773–783.

10. Brown G, Richards CJ, Bourne MW, et al. Morphologic predictors of lymph node status in rectal cancer with use of high-spatial-resolution MR imaging with histopathologic comparison. Radiology 2003;227:371–377.

11. Will O, Purkayastha S, Chan C, et al. Diagnostic precision of nanoparticle-enhanced MRI for lymph-node metastases: a meta-analysis. Lancet Oncol 2006;7:52–60.

12. Lahaye MJ, Engelen SME, Kessels AGH, et al. USPIO-enhanced MR imaging for nodal staging in patients with primary rectal cancer: predictive criteria. Radiology 2008;246:804–811.

13. Suppiah A, Hunter IA, Cowley J, et al. Magnetic resonance imaging accuracy in assessing tumour down-staging following chemoradiation in rectal cancer. Colorectal Dis 2009; 11:249–253.

14. Koh DM, Chau I, Tait D, Wotherspoon A, Cunningham D, Brown G. Evaluating mesorectal lymph nodes in rectal cancer before and after neoadjuvant chemoradiation using thin-section T2-weighted magnetic resonance imaging. Int J Radiat Oncol Biol Phys 2008;71:456–461.

15. Maretto I, Pomerri F, Pucciarelli S, et al. The potential of restaging in the prediction of pathologic response after preoperative chemoradiotherapy for rectal cancer. Ann Surg Oncol 2007;14:455–461.

16. Chen CC, Lee RC, Lin JK, Wang LW, Yang SH. How accurate is magnetic resonance imaging in restaging rectal cancer in patients receiving preoperative combined chemoradiotherapy? Dis Colon Rectum 2005;48: 722–728.

17. Harisinghani MG, Dixon WT, Saksena MA, et al. MR lymphangiography: imaging strategies to optimize the imaging of lymph nodes with ferumoxtran-10. RadioGraphics 2004; 24:867–878.

18. Harisinghani MG, Barentsz JO, Hahn PF, et al. MR lymphangiography for detection of minimal nodal disease in patients with prostate cancer. Acad Radiol 2002;9(suppl 2):S312–S313.

19. Heald RJ. A new approach to rectal cancer. Br J Hosp Med 1979;22:277–281.

20. DeLong ER, DeLong DM, Clarke-Pearson DL. Comparing the areas under two or more correlated receiver operating curves: a nonparametric approach. Biometrics 1988;44: 837–845.

21. Cohen J. A coefficient of agreement for nominal scales. Educ Psychol Meas 1960; 20:37–46.

22. Cohen J. Weighted kappa: nominal scale agreement with provision for scaled disagreement or partial credit. Psychol Bull 1968;70:213–230.

23. Shrout PE, Fleiss JL. Intraclass correlations: uses in assessing rater reliability. Psychol Bull 1979;86:420–428.

24. Landis JR, Koch GG. The measurement of observer agreement for categorical data. Biometrics 1977;33:159–174.

25. Kuo LJ, Chern MC, Tsou MH, et al. Interpretation of magnetic resonance imaging for locally advanced rectal carcinoma after preoperative chemoradiation therapy. Dis Colon Rectum 2005;48:23–28.

26. Habr-Gama A, Perez RO, Proscurshim I, et al. Absence of lymph nodes in the resected specimen after radical surgery for distal rectal cancer and neoadjuvant chemoradiation therapy: what does it mean? Dis Colon Rectum 2008;51:277–283.

27. Koh DM, Brown G, Temple L, et al. Rectal cancer: mesorectal lymph nodes at MR imaging with USPIO versus histopathologic findings—initial observations. Radiology 2004; 231:91–99.

28. Capirci C, Rubello D, Chierichetti F, et al. Restaging after neoadjuvant chemoradiotherapy for rectal adenocarcinoma: role of F18-FDG PET. Biomed Pharmacother 2004; 58:451–457.

29. Kristiansen C, Loft A, Berthelsen AK, et al. PET/CT and histopathologic response to preoperative chemoradiation therapy in locally advanced rectal cancer. Dis Colon Rectum 2008;51:21–25.

30. Abdel-Nabi H, Doerr RJ, Lamonica DM, et al. Staging of primary colorectal carcinomas with fluorine-18 fluorodeoxyglucose whole-body PET: correlation with histopathologic and CT findings. Radiology 1998;206:755–760.

31. Llamas-Elvira JM, Rodriguez-Fernandez A, Gutierrez-Sainz J, et al. Fluorine-18 fluorodeoxyglucose PET in the preoperative staging of colorectal cancer. Eur J Nucl Med Mol Imaging 2007;34:859–867.

32. Borschitz T, Wachtlin D, Mohler M, Schmidberger H, Junginger T. Neoadjuvant chemoradiation and local excision for T2-3 rectal cancer. Ann Surg Oncol 2008; 15:712–720.

33. O'Neill BD, Brown G, Heald RJ, Cunningham D, Tait DM. Non-operative treatment after neoadjuvant chemoradiotherapy for rectal cancer. Lancet Oncol 2007;8:625–633.